JOURNAL OF APPLIED ELECTROCHEMISTRY 11 (1981) 103–110

In situ evaluation of container corrosion in sodium–sulphur batteries

B. DUNN, M. W. BREITER, D. S. PARK

General Electric Corporate Research and Development, P.O. Box 8, Schenectady, NY 12301, USA

Received 31 March 1980

Recent improvements in container materials for Na/S cells (central sodium type) have led to greatly enhanced cell life and performance. Although problems with rapidly decreasing capacity are no longer observed, cells appear to exhibit a slowly increasing resistance with time. This paper describes an *in situ* technique for assessing the electrical stability of various container materials and determining the extent that corrosion processes influence cell resistance changes. Potentials within the sulphur electrodes of operating cells were measured over prolonged cycling times. Results indicate that chromized steel possesses excellent electrical stability compared to 347 stainless steel and that container corrosion accounts for only a fraction of the increase in total cell resistance.

1. Introduction

The long-term performance of Na/S cells (central sodium type) is seriously affected by corrosion of the sulphur container [1–3]. Formation of solid metal sulphides reduces the amount of available sulphur and disrupts electrical contact between the container and the carbon fibre matrix [3]. The latter can be particularly harmful because inadequate electronic contact results in ionic currents which, in turn, increase the corrosion rate [4]. Corrosion products may accumulate and hinder transport processes, as well as interact with the solid electrolyte and contribute to its degradation [5]. These corrosion-related factors serve to diminish cell performance as evidenced by a substantial decrease in utilization, of the order of 50%, within 200–300 cycles [6].

In recent years advancements in sulphur container materials have led to greatly reduced scale formation and considerable enhancement of long-term cell behaviour [4, 7]. Time-dependent effects have become more subtle. Increases in total cell resistance still occur though with only a small loss in cell capacity [7]. Although this represents a marked improvement, the rise in cell resistance has detrimental implications for large-scale energy storage systems. This paper attempts to determine the extent to which corrosion processes influence such cell resistance changes. An *in situ* technique was employed to measure potentials within the sulphur electrode of operating Na/S cells over the lifetime of these cells. Bones and Markin [6] used a similar approach to observe corrosion phenomena in 316 stainless steel. The results of the present study enable time-dependent changes occurring within the monitored section (i.e., the container and the region directly adjacent to it) to be compared for different cell casing materials and with overall cell characteristics. Information regarding the electrical stability of various container materials and the corresponding influence on total cell resistance is obtained.

2. Experimental

The experimental cell (Fig. 1) incorporated most of the standard components of the 16 A h laboratory cell [7]. A notable addition was a thin molybdenum wire (0.5 mm diameter) which was glass sealed to an alumina insulator at the bottom of the container. A mechanical seal fastened this header to the container thus closing the bottom of the cell. The molybdenum probe was placed approximately at the midpoint of the sulphur electrode and was in contact with both the melt and the carbon mat (conductive mat region [8]). The probe was electronic when the cell cycled in the

0021–891X/81/010103–08$02.80/0

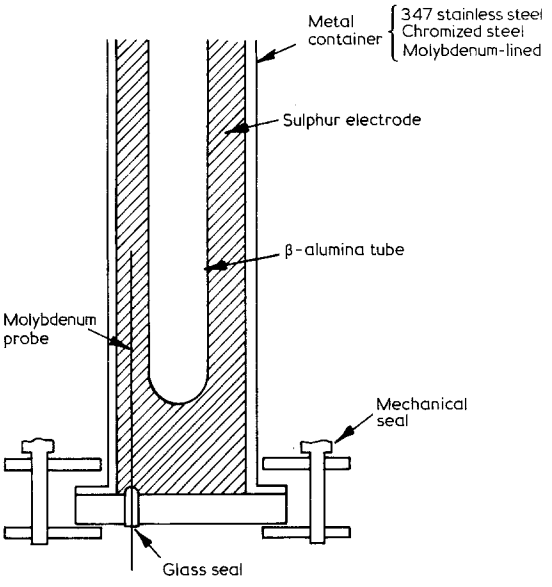

Fig. 1. Lower part of Na/S cell indicating the placement of the probe within the sulphur electrode.

two-phase region, as indicated by an open-circuit voltage of < 1 mV between the probe and the container. In the one-phase region a mixed electronic and ionic potential was recorded.

The cells tested in this study had three different container materials: (a) 347 stainless steel, (b) molybdenum-lined 347 stainless steel and (c) chromized steel. The molybdenum liner was prepared by rolling foil (0.002 inch thick) into a cylinder of the required diameter and length, inserting it into the container and spot welding the foil circumferentially at the top, bottom and along the seam. The technique effectively prevents the melt from seeping between the foil and casing. Recent results with cells using molybdenum containers show corrosion behaviour virtually identical to that found with molybdenum-lined containers [9]. Chromized steel is a recently developed sulphur container material which displays excellent corrosion resistance [7]. These pore-free, diffusion-bonded coatings are prepared by a pack cementation process at elevated temperatures. The chromized steel used in this study had a surface chromium level in excess of 70 wt%.

The potential difference between the probe and the container was measured continuously as the cell cycled. Specific cell cycling procedures have been described previously [8]. The potential difference as measured contains contributions from the following elements of the Na/S cell: (a) the corrosion layer on the container, (b) contact between the container and the carbon mat and (c) a section of the melt–carbon mat matrix. Although the method does not definitively distinguish among the three contributions, it does provide a means for continuously monitoring the region of primary interest during actual cell cycling. Over extended cycling time, changes in the potential drop between container and probe can be associated with resistance changes in the monitored section. The information may then be compared with the other containers and with resistance changes in the total cell. Furthermore, the molybdenum-lined container represents a control sample. The excellent corrosion resistance of molybdenum not only makes it a logical choice as the probe material (thus enabling contributions from probe corrosion to be minimized) but also provides a standard upon which to compare the corrosion behaviour of other case materials. In addition the molybdenum-lined container represents a situation where at least one of the contributions to the measured potential difference (certainly the corrosion process and perhaps the contact resistance) is negligible.

3. Results

General aspects of the cycling performance for the experimental cells are shown in Table 1 at comparable stages of cell life. The values for cell life are referred to the area of the solid electrolyte (20 cm^2). 2.4 A h cm^{-2} corresponds to one day of cycling, so that cell 410 was cycled continuously for six months. Cell 449 was terminated because of an electrical failure, the other cells were removed voluntarily. Decline in utilization for the stainless steel cell with eventual operation in only the one-phase region has been reported previously [1]. The other cells charge well into the two-phase region, although the decrease observed for the chromized steel case is rather atypical. Utilization of 70–75% is more commonly observed at longer cell lifetimes [7]. In all three cells, total cell resistance increases rather persistently. This increase prevents the cell from recharging fully because of the voltage limit preset for cycling at constant current. Such behaviour represents the primary means for capacity loss in cells such as 410 and

Table 1. Cycling performance of tested cells

Cell	*Container material*	*Cycle*		*Cell life* ($A\,h\,cm^{-2}$)	*Per cent utilization*
391	347 stainless steel		5	6	83.6
			100	109	90.6
			250	253	70.0
		Last	415	366	37.3
410	Chromized steel		5	6	88.7
			100	111	80.7
			242	256	73.4
		Last	470	438	60.0
449	Molybdenum-lined steel		5	5	93.7
			100	110	84.0
			195	235	77.5
		Last	245	264	81.9

449. Cells with stainless steel containers have additional contributions arising from a reduction of available sulphur through corrosion and through isolation of electrode segments [1].

3.1. *Responses of the potential probe*

The *in situ* measurement of the potential difference between probe and container was designed to determine whether the increase in resistance occurring within the cells was located at the container or at the region immediately adjacent to it. In Figs. 2–4 the potential difference $\phi_c - \phi_p$ between the container and the probe is shown for various cycles of the three different cells. The points represent the open-circuit voltage (V_{oc}). In the two-phase region, i.e., at the beginning of the discharge of cycle 10 in Fig. 2, V_{oc} is about 1 mV, an indication that the potential is virtually all electronic. Since contributions from the composition gradients within the electrode arise in the one-phase region, V_{oc} varies accordingly. However, the presence of substantial values for V_{oc} in the two-phase region is evidence of residual polysulphide and supports the hypothesis that certain regions of the sulphur electrode are isolated and do not contribute to cell capacity [1]. This behaviour was observed for the stainless steel cell container at later cycles but not for the other containers, an indication that the large V_{oc} values are associated with significant changes occurring within the monitored section of the stainless steel cell.

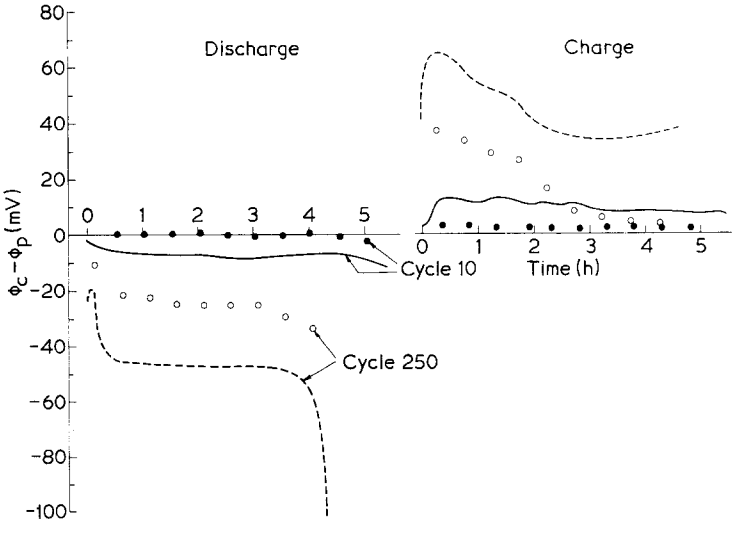

Fig. 2. Voltage between container and probe for discharge and charge cycles 10 and 250 for cell 391 with stainless steel container.

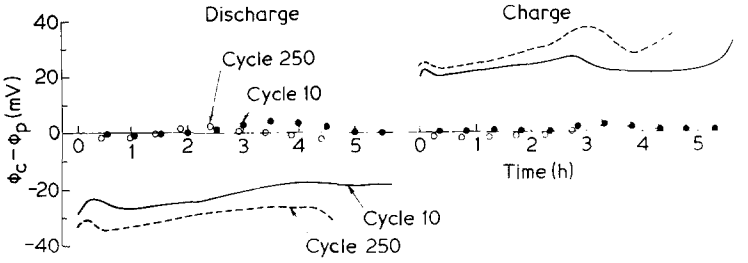

Fig. 3. Voltage between container and probe for discharge and charge cycles 10 and 250 for cell 410 with chromized steel container.

There are two considerations in interpreting the voltage traces: the curve shape for a given cycle and the change in magnitude (and shape) over the life of the cell. The former is associated with electrochemical processes occurring within the monitored segment as a function of the state of charge, i.e., as a function of composition. Corrosion would appear to be the primary electrochemical reaction since voltammetric studies [10] and a.c. impedance measurements [11] indicate that Na/S cells operate well within the linear regime of the carbon–sodium polysulphide current–potential curve. Thus the structure of the voltage traces can be related to container corrosion. However, because there are also contributions from the reversible potential of the system, direct correlation with specific reactions is difficult. Variations in the magnitude of the trace represent a change in the resistance between container and probe. Possible sources include the corrosion scale, the scale–carbon mat interface and the carbon mat–sodium polysulphide electrode.

The curves for cell 391 (stainless steel container) exhibit two distinguishing features (Fig. 2). At the very end of the discharge an abrupt increase in the potential difference occurs which becomes more prominent with increasing cycle life. The charge cycle displays a broad peak during the early stages of charging, i.e., in the one-phase region, but apparently not at the composition Na_2S_3. It is interesting to note that these two features are fairly consistent with the corrosion behaviour of a similar stainless steel (316) reported by Bones *et al.* [12]. Under polarizing conditions in the presence of carbon felt, film stripping was observed at the end of discharge while adherent corrosion layers were formed during the charge cycle (although not at $Na_2S_{3.6}$) and the remainder of discharge. Although this is an interesting correlation, it cannot be considered definitive. The voltage traces observed during the early stages of cycling are comparable in shape and magnitude to those reported previously [6]. After extended cycling there is an obvious increase in the magnitude of the potential drop (Fig. 2). This reflects an increase in resistance within the monitored area, an item which is discussed in detail later. In addition the open-circuit voltage at the beginning of the discharge in cycle 250 is an indication of residual polysulphide and that there are sections of the sulphur electrode which are not contributing to cell capacity.

The behaviour of cells 410 and 449 (chromized steel and molybdenum-lined containers respectively) is virtually identical. The potential difference $\phi_c - \phi_p$ varies by only a few millivolts throughout the entire length of the cycle, a feature due probably to changes in the reversible potential as a function of composition and, perhaps, concentration polarization [13]. Thus, in comparison to the stainless steel cell, these two cells do not appear to exhibit the type of voltage trace associated with corrosion reactions. Furthermore, there is very little change in magnitude with cycling time,

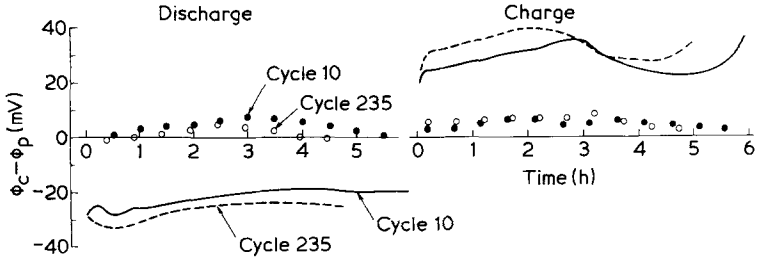

Fig. 4. Voltage between container and probe for discharge and charge cycles 10 and 235 for cell 449 with molybdenum-lined container.

another indication of corrosion stability. Morphological examination confirms the electrochemical results as discussed below. The relatively constant values for $\phi_c - \phi_p$ also suggest that the contact resistance between the container and the carbon mat remains at a uniform level throughout cycling.

3.2. *Time-dependent behaviour*

The resistance increase with time is shown in a more quantitative fashion for the three cells in Fig. 5. The ordinate V_{cor} is corrected for the measured open-circuit voltage $(\phi_c - \phi_p)_0$ between the probe and container. The resulting quantity minimizes contributions which arise from concentration polarization and enables the ohmic portion to be more accurately resolved. For chromized steel and molybdenum, this correction amounts to only a few millivolts and has little effect. In cell 391, however, the contribution is fairly substantial. The abscissa is a measure of cell lifetime. All data were taken on discharge (25 cycle intervals) at the same state of charge (12 A h) corresponding to a composition of approximately Na_2S_4. This latter procedure was aimed at normalizing contributions from the polysulphide melt.

The three container materials exhibit rather interesting behaviour. After an incubation period of approximately 2000 A h (or 100 A h cm^{-2}), the stainless steel and chromized steel cells display a monotonic increase which is parabolic in time. The larger slope of the stainless steel is an indication of the poorer corrosion resistance it possesses in comparison with the other materials. The slope would be even greater if the ionic portion of the potential drop were included in the calculation. The greatly reduced slope for chromized steel and molybdenum is consistent with the voltage traces in Figs. 3 and 4 and their respective corrosion behaviour in Na/S cells. Unfortunately, the somewhat abbreviated life of cell 449 prevented an accurate determination of its slope over prolonged cycling times.

3.3. *Corrosion morphology*

The conclusions based on the potential difference measurements are confirmed by post-operative examinations of cell casings. Table 2 summarizes the salient physical characteristics as derived from these studies. The 347 stainless steel casings exhibit fairly extensive scale formation, although actual thicknesses are quite variable [14]. The thick corrosion product accumulated adjacent to the container can be easily removed, exposing a shiny metallic substrate (Fig. 6). In contrast chromized steel and molybdenum containers exhibit thin, adherent corrosion layers. There are some local variations in thickness as indicated in Table 2; however, the layers are generally quite

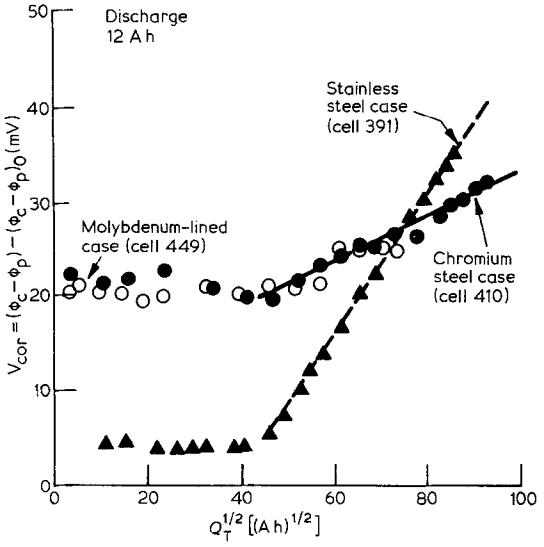

Fig. 5. Potential difference (corrected for the open-circuit voltage) at 12 A h discharge as a function of cell lifetime for each of the cells.

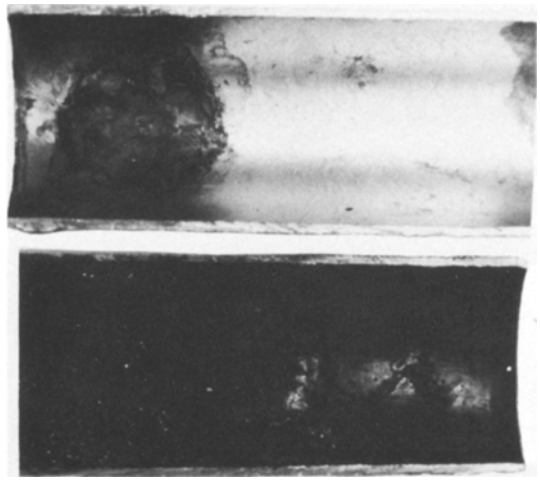

Fig. 6. Morphology of 347 stainless steel container for cell 162 (~ 10 400 A h). The black, emulsion-like scale (below) can be lifted off to reveal a shiny, metallic surface.

Table 2. Physical characteristics of container corrosion from post-operative examination

	347 stainless steel	*Chromized steel*	*Molybdenum*
Phases	FeS_2 and traces of NiS_2, Cr_2S_3, Cr_3S_4, $FeCr_2S_4$	Cr_2S_3	MoS_2
Morphology	Non-adherent scale, emulsion-like appearance. Shiny surface underneath the scale. Variable thickness.	Very uniform, adherent	Very adherent. Local thickness variations.
Thickness (10 000 A h)	50–200 μm. Poor reproducibility.	0.5–2 μm	2–6 μm

uniform. Corrosion stability of chromized steel is shown in Fig. 7 for a cell which had accumulated over 13 000 A h (650 A h cm^{-2}). The outside surface (Fig. 7b) was in contact with the ambient atmosphere at 315° C. Under these conditions there is virtually no reaction and thus Fig. 7b represents the initial microstructure. Comparison of this surface with the one in contact with molten sulphur and sodium polysulphides (Fig. 7a) indicates that very little corrosion has occurred. From additional cells and separate corrosion studies, it is estimated that this layer is no more than 2 μm thick. The primary phase identified by X-ray diffraction is Cr_2S_3. The behaviour of molybdenum is analogous to that of chromized steel. Morphology, thickness and scale composition on stainless steel and molybdenum are consistent with results at other laboratories [4, 15]. Analytical studies of chromized steel as a sulphur container for Na/S cells have not yet been reported.

Another interesting feature observed from the post-operative examinations was the nature of the contact between the carbon mat and the cell container. With 347 stainless steel, the excessive accumulation of corrosion products results in the loss of direct contact between the carbon mat and the container, an effect well known with this material [1, 3, 14]. On the other hand both chromized steel and molybdenum-lined casings have fibres directly attached to the container. Scanning electron microscopy indicates that the fibres are attached at the surface and do not penetrate the sulphide scale. These morphological observations strongly suggest that contact between the carbon mat and either the chromized steel or molybdenum-lined containers is maintained throughout prolonged cell cycling, a conclusion which was also reached on the basis of the potential difference measurements for these materials.

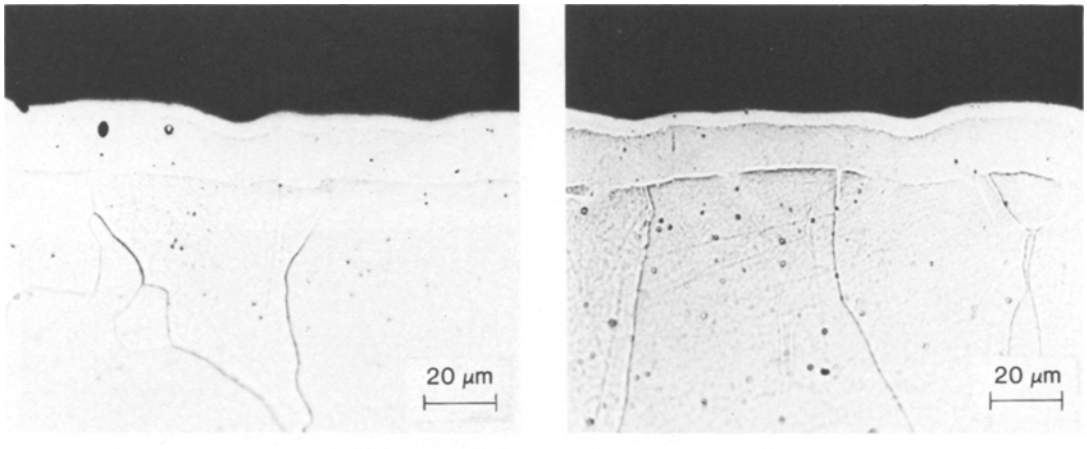

Fig. 7. Cross-section of chromized steel container for cell 356 (~ 13 000 A h). Very little corrosion is evident although the appearance normal to the surface is that of a uniform black layer. See text for discussion of (a) and (b).

4. Discussion

The present work provides information concerning two important areas: the electrical stability of container materials and the effect of corrosion-related phenomena on total cell resistance. Data were obtained directly from operating cells, an obvious benefit of the *in situ* technique. The results concerning net corrosion behaviour are fairly definitive. Chromized steel exhibits excellent electrical stability and represents a considerable improvement over stainless steel. Molybdenum is certainly comparable to chromized steel and perhaps slightly better. The excellent corrosion behaviour of molybdenum containers confirms the results of previous investigations. Physical characterization from post-operative examinations of cell casings are completely consistent with the potential difference measurements and supports the conclusions.

Although the corrected potential difference in Fig. 5 contains contributions from contact resistances, the sulphur electrode and container corrosion, it appears that time-dependent behaviour is primarily due to the latter. This inference can be drawn because of the use of molybdenum in cell 449. The thin, adherent, corrosion-resistant scale which forms enables cell 449 to be considered as a control sample. Cell corrosion processes are minimized and contact between the carbon fibre matrix and the container wall remains virtually constant throughout the life of the cell. Thus the observed increase in V_{cor} for cell 391 strongly suggests that corrosion is responsible for this behaviour, since V_{cor} for the corrosion-resistant material remains nearly constant. The parabolic increase with time is consistent with corrosion depth studies reported for 316 stainless steel [15]. However, it should be noted that the corrosion behaviour of 347 stainless steel exhibits considerable variation in corrosion rate [14]. Extending this analysis to chromized steel is less valid because cell 449 did not cycle sufficiently to determine whether V_{cor} truly exhibits an increase over prolonged cycling time. A detailed kinetic study of the corrosion of chromized steel is in progress.

The other significant result derived from this study concerns the extent to which the corrosion resistance influences the increase in total cell resistance. A direct comparison is possible because the cell cycles at constant current. Table 3 compares the total increase in resistance of cell 391 (stainless steel container) with that derived from the potential difference measurements for all three cells. The behaviour of cell 391 is quite representative since similar magnitudes of resistance increase were observed for cells 410 and 449. It is clear that the added container resistance (obtained by subtracting the average incubation period values from the ones measured at later stages of cell life) produces only a fraction of the rise observed for the entire cell. This occurs even with the 347 stainless steel casing which is the most susceptible to corrosion and exhibits the largest resistance increase. These results indicate that the primary source of the rise in cell resistance is not associated with the container (and corresponding contact resistance) and that other cell components are largely responsible.

Table 3. Resistance increase with cycling time

	Cell life (A h)				
	1500	*3000*	*4500*	*6000*	*7000*
Total cell (cell 391)	9.5 mΩ	32 mΩ	49 mΩ	63 mΩ	72 mΩ
Stainless steel container	0	4.0	8.0	12.5	14.5
Chromized steel container	0	0	2.0	3.0	3.9
Molybdenum-lined container	0	0	1.8	*	*

* Cell failed at 5200 A h.

Acknowledgements

The authors are very grateful to F. G. Malone for experimental assistance and to T. M. Evenden for data reduction. The work was supported in part by the Electric Power Research Institute.

References

[1] I. Wynn Jones, *Electrochim. Acta* **22** (1977) 681.
[2] M. W. Breiter, J. B. Bush, Jr., S. P. Mitoff, O. Muller and W. L. Roth, 'Proc. Energy Storage Symp.', The Electrochemical Society, Princeton (1976) p. 165.
[3] M. P. J. Brennan, *J. Electrochem. Soc.* **125** (1978) 705.
[4] B. Hartmann, *J. Power Sources* **3** (1978) 227.
[5] R. P. Tischer and F. A. Ludwig, 'Advances in Electrochemistry and Electrochemical Engineering', vol. 10 (edited by H. Gerischer and C. W. Tobias) John Wiley, New York (1977) p. 391.
[6] R. J. Bones and T. L. Markin, *J. Electrochem. Soc.* **125** (1978) 1587.
[7] Electric Power Research Institute, Interim Report, EM-683, Project 128-4 (1978).
[8] D. Chatterji, S. P. Mitoff and M. W. Breiter, 'Proc. Load Leveling Symp.', The Electrochemical Society, Princeton (1977) p. 251.
[9] D. S. Park and M. W. Breiter, unpublished results.
[10] R. D. Armstrong, T. Dickinson and M. Reid, *Electrochim. Acta* **20** (1975) 709.
[11] M. W. Breiter and B. Dunn, *J. Appl. Electrochem.* **9** (1979) 671.
[12] R. J. Bones, R. J. Brook and T. L. Markin, in 'Power Sources' vol. 5 (edited by D. H. Collins) Academic Press. London (1975) p. 539.
[13] M. P. J. Brennan, *Electrochim. Acta.* **24** (1979) 529.
[14] D. S. Park, M. W. Breiter and D. Chatterji, to be published.
[15] Department of Energy, Final Report, Contract No. EY-76-C-02-2566 (1977).